

Fracture Toughness of a 6061Al Matrix Composite Reinforced with Fine SiC Particles

Lihe Qian^{1,2,*}, Toshiro Kobayashi², Hiroyuki Toda², Takashi Goda² and Zhong-guang Wang¹

¹Shenyang National Laboratory for Materials Science, Institute of Metal Research, Chinese Academy of Sciences, Shenyang 110015, P.R. China

²Department of Production Systems Engineering, Toyohashi University of Technology, Toyohashi 441-8580, Japan

The fracture toughness of 6061Al alloy metal matrix composite reinforced with 15 vol% fine SiC particles of 600 nm in size under a high temperature over-aged condition was studied. And the toughness of the 6061Al matrix alloy and the same matrix alloy reinforced with coarse SiC particles of 9.5 μm were also measured for comparison. Fracture toughness tests were conducted on a servo-hydraulic testing machine by using three point bending specimens. The results showed that the toughness of the fine particle reinforced composite was obviously higher than that of the coarse particle reinforced composite in terms of crack initiation toughness, crack propagation energy and total absorbed energy. The mechanisms controlling the fracture toughness of the two composites reinforced with fine and coarse SiC particles were discussed based upon the measured toughness data and microstructure examinations by means of an optical microscope and a scanning electron microscope.

(Received May 7, 2002; Accepted September 11, 2002)

Keywords: fracture toughness, composites, metal matrix composite

1. Introduction

The mechanical behavior of particle-reinforced aluminum metal matrix composites has been extensively studied since they have enhanced strength and stiffness over their monolithic alloys at room and elevated temperatures, and are relatively isotropic and easier to fabricate compared to continuous fiber-reinforced metal matrix composites. However, it has been demonstrated that addition of particles can drastically degrade the ductility and fracture toughness of the composite materials. The characters of particles play an important role in controlling the toughness of the composites, and the degradation of toughness is considered to be due to cracking of particles, nonuniformity of particles and changes in matrix flow behavior.¹⁻³⁾ It was commonly observed that an increase in volume fraction of SiC_p would decrease fracture toughness of the composite, which is consistent with some published findings⁴⁾ and our previous reports.^{5,6)} On the other hand, an increase in SiC particle size would increase the fracture toughness, which has been confirmed by Kamat's research⁷⁾ and Davidson's result.²⁾ In their work, the studied SiC particle size was larger than 2 μm . However, how particles of even finer size (smaller than 1 μm) affect the fracture toughness of the composite has not been clarified experimentally. In addition, previous researches were focused on the properties of the composites in under aged (UA), T6 or normal temperature over aged (OA) conditions.^{2,4)} Nevertheless, a high temperature OA state is inevitably encountered in practical applications, which has not been investigated yet. This paper presents the results of a comparative study of the fracture toughness of fine or coarse SiC particle reinforced 6061Al (Al-0.75Mg-0.68Si-0.29Cu-0.20Fe-0.14Zn) alloy matrix composites of same particle volume fraction in a high temperature OA condition.

2. Experimental

The 6061Al alloy metal matrix composite reinforced with 15 vol% fine SiC particles of 600 nm in size were fabricated by a method of vortex melting followed by squeeze casting.⁸⁾ First, molten 6061Al alloy at 750°C was stirred with preheated SiC particles at a stirring speed of 500–800 rpm in a crucible for 10.8 ks. Then, the as-cast composite ingot with size of $\phi 65 \times 130$ mm was further formed at 850°C in an air atmosphere under a pressure of 100 MPa using a squeezing machine in order to remove the defects. The 6061Al matrix alloy and the same matrix alloy reinforced with coarse SiC particles of 9.5 μm , made by the same routine as the fine particle reinforced composite, were adopted as a comparison. All the composite materials were solution heat treated at 520°C for 7.2 ks, quenched by water, peak-aged at 190°C for 25.2 ks, and then overaged at 300°C for 86.4 ks. The 6061Al matrix alloy was heat treated in the same way as composites except peak-aged at 190°C for 3.6 ks. Three point bending specimens of 10 mm \times 10 mm \times 55 mm in size, were used for the fracture toughness tests. All specimens were first mechanically cut and then pre-fatigued to a crack length of around 5 mm (cut length plus fatigued length) using step-by-step decreasing load method according to ASTM standard.⁹⁾ The experiments were conducted at room temperature on a servo-hydraulic testing machine. Load-deflection curves of different materials were recorded and the apparent crack initiation toughness J_{IC-a} , was evaluated according to Rice's equation:

$$J_{IC-a} = 2E_M/B(W - a_0) \quad (1)$$

where E_M is the energy consumed until the maximum load, B the specimen thickness, W the specimen width, and a_0 the initial crack length. The exact value a_0 was measured using a low magnification microscope after fracturing the specimen according to ASTM standard.⁹⁾ Their crack propagation energies E_P and the total absorbed energies E_T normalized by $B(W - a_0)/2$ were also compared. The topography of frac-

*Present address: Institute of Industrial Science, The University of Tokyo.

tured specimens and the microstructure beneath fracture surfaces were examined in detail using a scanning electron microscope (SEM) and an optical microscope (OM) respectively to characterize the fracture mechanisms of the studied composites.

3. Results

Three tests were performed and corresponding three load-deflection curves were recorded for each material. A typical load-deflection curve of the studied fine composite is plotted in Fig. 1, and compared with those of the contrast materials. The results of the fracture toughness determined from load-deflection curves are given in Table 1 and illustrated in Fig. 2 with error bars. It can be clearly noted that the apparent crack initiation toughness, crack propagation energy and total absorbed energy of both fine and coarse composites are all much lower than those of 6061Al alloy. Comparison between the two composites indicates that the fine particle reinforced composite shows obviously higher values than the composite reinforced with coarse particles, with an increase of about 30% in terms of all the three fracture toughness parameters.

The typical SEM fractographs of the crack initiation zones ahead of the pre-fatigued crack tips are respectively shown in Fig. 3 for the fine particle reinforced composite, and in Fig. 4 for the coarse particle reinforced composite. Both fractographs are characterized by dimple morphology, indicating ductile fracture. However there are differences between the two kinds of micrographs. For the coarse SiC reinforced composite, there are two groups of dimples as described in 6): a group of large dimples and a group of small dimples. The

group of large dimples are around $10\mu\text{m}$ in size, probably related with SiC particles since average SiC particle size is about $9.5\mu\text{m}$. This is further confirmed by some particles contained in dimples as indicated by arrows in Fig. 3. Another group of dimples are much smaller, around $1\mu\text{m}$, so it should be associated with precipitates and inclusions in the

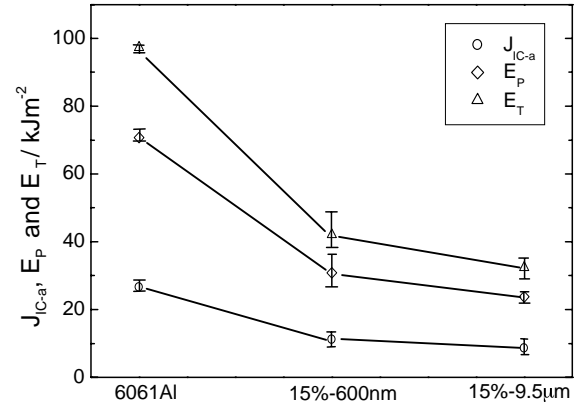


Fig. 2 Apparent crack initiation toughness J_{IC} , crack propagation energy E_P and total absorbed energy E_T of SiCp/6061Al composites and their matrix alloy. Note that E_P and E_T are normalized by $B(W - a_0)/2$.

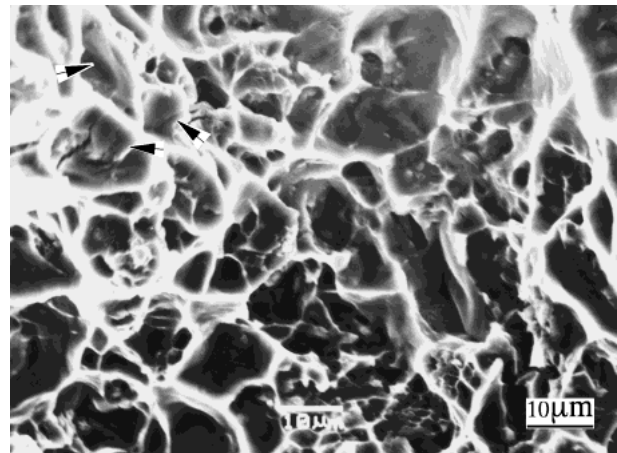


Fig. 3 Typical fractograph of the crack initiation zone for $9.5\mu\text{m}$ SiCp/6061Al. Arrows indicate particles lying in dimples.

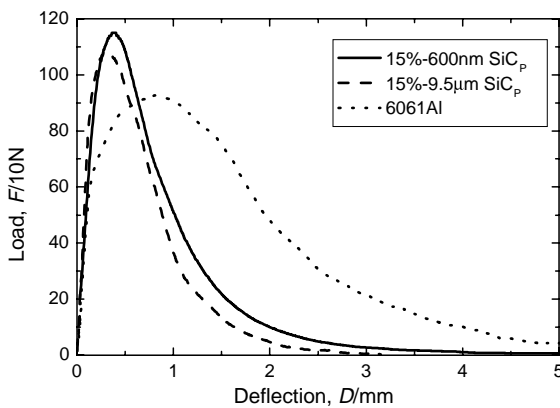


Fig. 1 Representative load-deflection curves of SiCp/6061Al composites and their matrix alloy under fracture toughness tests.

Table 1 Measured fracture properties of SiCp/6061Al composites and their matrix alloy.

Material	Initiation energy, J_{IC-a}/kJm^{-2}	Propagation energy, E_P/kJm^{-2}	Total energy, E_T/kJm^{-2}
0.6 μm SiCp	11.3	30.8	42.1
9.5 μm SiCp	8.65	23.8	32.4
6061Al	26.6	70.7	97.3

Values are averages of three measurements. E_P and E_T are normalized by $B(W - a_0)/2$.

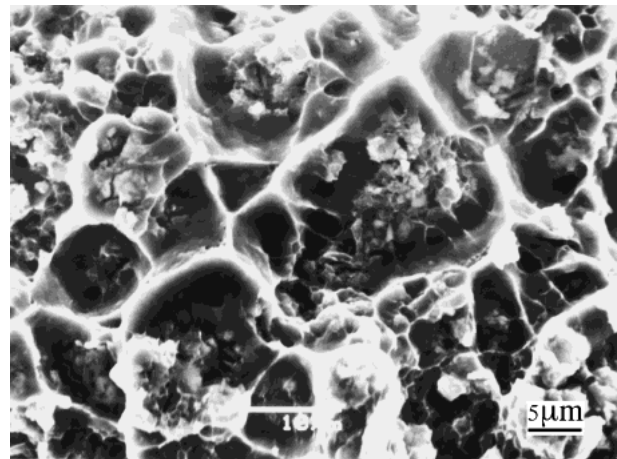


Fig. 4 Typical fractograph of the crack initiation zone for 600nm SiCp/6061Al. Large dimples are composed of small dimples in the bottoms.

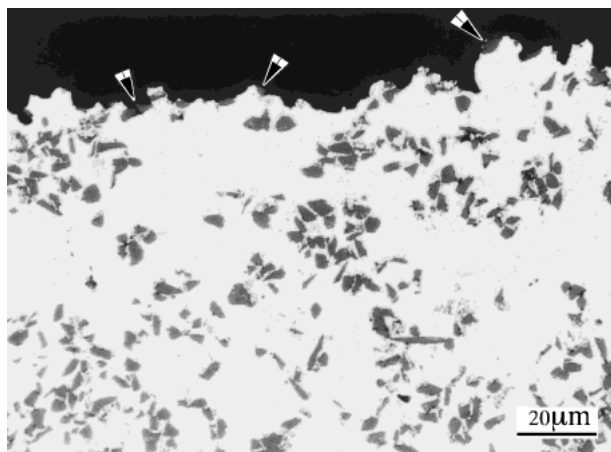


Fig. 5 Microstructure beneath fracture surface of 9.5 μm SiCp/6061Al. Some exposed particles are seen and indicated by arrows.

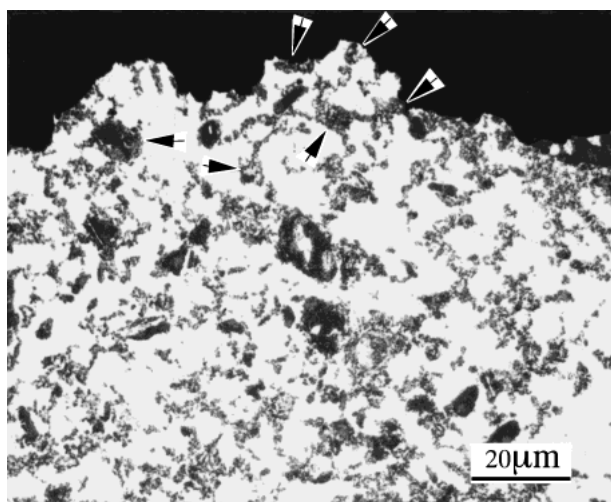


Fig. 6 Microstructure beneath fracture surface of 600 nm SiCp/6061Al. Some typical clusters on or under the fracture surface are indicated by arrows.

material as indicated in 6). Whereas for the fine SiC particle reinforced composite, also a lot of large dimples exist, however, nearly all the large dimples are composed of small dimples in the bottoms, making the bottoms of the larger dimples deeper and coarser.

The representative microstructures adjacent to fracture surfaces are shown in Figs. 5 and 6 for the two composites. For the coarse particle reinforced composite, many SiC particles can be seen exposed on the fracture surface (Fig. 5). We can assume that the fracture of coarse particle reinforced composite is due to the crack initiation and growth in the matrix around SiC particles. This is verified in Fig. 7. Figure 7 is a micrograph from an *in-situ* SEM observation in our previous research⁶⁾ on the same material as the composite reinforced with coarse particles in the present study. This photograph clearly demonstrates that voids initiated in the matrix subjected to severe plastic deformation around particles ahead of crack tip under three point bending. These voids grew along particles, coalesced with nearby voids and connected with the main crack. Nevertheless, it is indicated in Fig. 6 that the fine SiC particles distributed nonuniformly with cluster colonies here and there. The crack path along the fracture surface

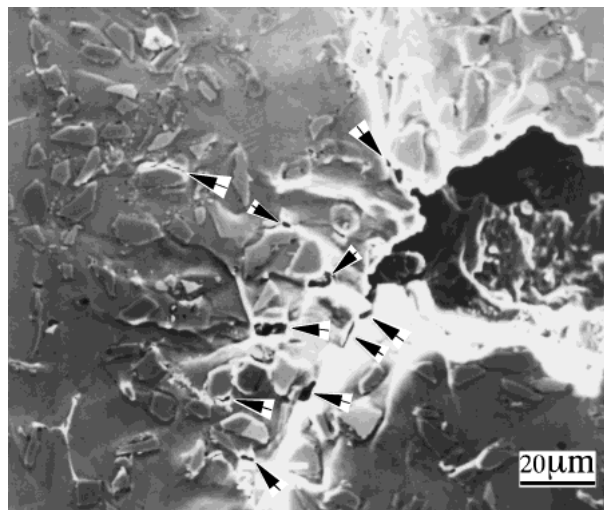


Fig. 7 *In-situ* SEM micrograph (from literature 6) showing voids (indicated by arrows) formed around particles within heavily deformed region ahead of fatigued crack tip (right) under three point bending.

(Fig. 6) demonstrates that the boundaries between the particle clusters and surrounding matrix might play an important role in cracking. This is consistent with the dimple morphology shown in Fig. 4, where the small dimples contained in large dimples might result from the individual fine particles around a cluster.

4. Discussion

A model proposed by Rice and Johnson,¹⁰⁾ and later modified by Hahn and Rosenfield¹¹⁾ concerns the effect of particle size and volume fraction on fracture toughness. According to ductile rupture mechanism, Hahn and Rosenfield assumed that if a material contains a crack and is loaded the crack will propagate when the extent of the heavily deformed region ahead of the crack tip grows large enough and comparable to the unbroken ligament size separating the particles responsible for void initiation. They further assumed that all of the particles in the vicinity of crack tip are responsible for void nucleation by particle rupture, decohesion or severe plastic deformation in the matrix at reinforcement ends. And then, an equation was derived by Hahn and Rosenfield¹¹⁾ as follows:

$$K_{IC} = (2\sigma_y \lambda E)^{1/2} \quad (2)$$

where K_{IC} is the fracture toughness, σ_y the yield strength, λ the average spacing of all particles, and E the elastic modulus. λ can be calculated by $\lambda = (2\pi/3F_v)^{1/2} D/2$, where D is particle size, and F_v is volume fraction of the reinforcing particles. According to the relationship: $J_{IC} = K_{IC}^2(1 - \nu^2)/E$, where J_{IC} is J integral and ν is Poisson's ratio, Hahn and Rosenfeld's model can be rewritten to:

$$J_{IC}/2\sigma_y(1 - \nu^2) = \lambda \quad (3)$$

It is apparent that if Hahn and Rosenfeld's assumption is satisfied (*i.e.*, $J_{IC}/2\sigma_y(1 - \nu^2) = \lambda$ holds, as drawn in Fig. 8), coarse particle reinforced composites will show higher fracture toughness. This is not in agreement with present experimental results, where the fine particle composite shows higher fracture toughness. For the fine and coarse particle

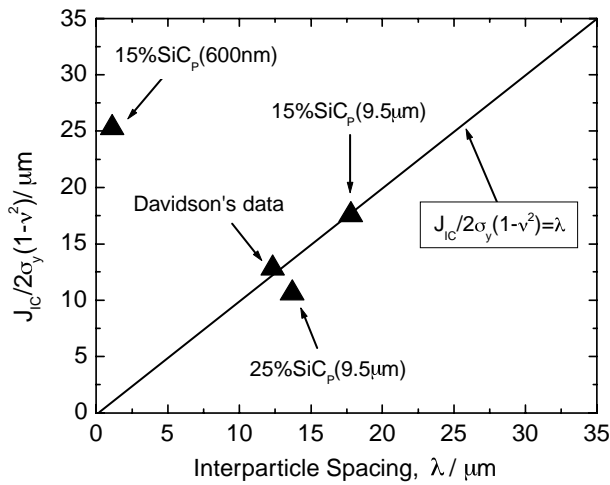


Fig. 8 Relationship between $J_{IC}/2\sigma_y(1 - v^2)$ and the average spacing of all the SiC particles in the composites.

composites in the present investigation, λ values are calculated to be $1.2 \mu\text{m}$ and $17.7 \mu\text{m}$, respectively. Input the measured data J_{IC-a} into $J_{IC}/2\sigma_y(1 - v^2)$, $J_{IC}/2\sigma_y(1 - v^2)$ are then plotted in Fig. 8 as a function of λ . Our previous result for 25% $9.5 \mu\text{m}$ SiC_p/6061Al⁶⁾ and Davidson's data²⁾ are also included in Fig. 8 for comparison. Clearly, the experimental data for both $9.5 \mu\text{m}$ SiC_p(15% and 25%)/6061Al and $6.6 \mu\text{m}$ SiC_p(15%)/2024Al lie on or close to the line drawn using eq. (3), hence satisfying the Hahn and Rosenfield's assumption. This suggests that all the SiC particles within the large plastic deformation zone in front of the crack tip are possible positions for void initiation. This is reasonable since the particles in the above composites are large in size so that particles are easy to crack, or debond from surrounding matrix, or initiate voids in the matrix around these particles ahead of the loaded crack tip. As demonstrated in Fig. 7, the matrix around particles ahead of the crack tip was subjected to severe plastic deformation, and voids indeed initiated in the matrix. Figure 7 also indicates that nearly all the particles engulfed by the plastic deformation zone ahead of pre-fatigued crack tip contribute to voiding, thus satisfying Hahn and Rosenfield's assumption.

However, the experimental data for the fine particle reinforced composite deviates largely from the line $J_{IC}/2\sigma_y(1 - v^2) = \lambda$, not satisfying Hahn and Rosenfield's model. According to eq. (3), for this fine particle composite with a toughness value of 11.27 kJ/m^2 (Table 1), the spacing between the possible sites for void initiation at the crack tip should be around $25 \mu\text{m}$. This value is far larger than the average spacing of all the particles in the composite, $1.2 \mu\text{m}$ (calculated above). Therefore, only a small part of the fine particles within the heavily deformed region ahead of the pre-fatigued crack tip are assumed to contribute to void initiation. It has already been known^{12,13)} that the smaller the size of the particles, the larger the stress for cracking or debonding of these particles. Broek¹⁴⁾ found that particles of 100 nm in size hardly cracked or debonded during deformation. He observed that fine particles formed dimpled voids only during formation of deformation band or during coalescence of voids after strain localization, which was not quite harmful to the material's fracture toughness. Similarly, the individual

particles of small size in the present composite may not deteriorate fracture toughness much. Therefore, the fact that only a small part of the fine particles in the present composite are responsible for the void initiation ahead of crack tip is consistent with the above published findings.¹²⁻¹⁴⁾ It follows that Hahn and Rosenfield's assumption cannot explain the higher fracture toughness of the fine particle reinforced composite compared with larger particle reinforced one.

It is well known that a material's toughness is decided by the energy consumption for fracturing the material. A metal or an alloy usually shows higher toughness because of more plastic deformation energy consumed at the crack tips before cracking. For a composite, however, addition of reinforcements decreases the toughness of its matrix. This decrease is a result of competition between the decreased energy consumption for plastic deformation and increased energy consumption for fracturing the reinforcements, debonding or separation between the reinforcements and surrounding matrix. Thus, the extent of decrease in toughness is largely dependent upon (1) the volume fraction and properties of the reinforcement, including its type, size and orientation; and (2) the material's processing routine, which affects the distribution of the reinforcements, and severity of segregation or clusters. It is reported that an increase in volume fraction of SiC_p would decrease fracture toughness,⁴⁻⁶⁾ and an increase in SiC particle size would increase the fracture toughness.^{2,7)} This is explained as follows. The more extensive unreinforced matrix regions surrounding the larger size reinforcements or reinforcements with less volume fraction will enhance the fracture toughness by producing more matrix plastic deformation. On the other hand, for a composite reinforced with much smaller reinforcements, these smaller particles behave as precipitates do. Energy consumption for voiding, debonding or separation between the reinforcements and surrounding matrix becomes larger, while plastic deformation energy is supposed to comparable with large particle reinforced composite. This may account for the higher fracture toughness of the fine particle reinforced composite measured in the present investigation. Further study is needed to investigate the effect of fine particles on fracture behavior of composite materials.

5. Conclusions

Based upon the above evaluation of the fracture toughness of the 6061Al metal matrix composite reinforced with 15 vol% fine SiC particles of 600 nm and comparison with that of coarse SiC particle reinforced composite, we conclude as follows:

- (1) The fine particle reinforced composite shows higher crack initiation toughness, crack propagation energy and total absorbed energy compared with the coarse particle reinforced composite.
- (2) The crack initiation and fracture of the coarse particle reinforced composite were mainly associated with voiding in the matrix around individual particles ahead of main crack tip, whereas the boundaries between the particle clusters and surrounding matrix may be responsible for the failure of the fine particle reinforced composite.

Acknowledgments

This work was subsidized with the special Funds for the Major State Basic Research Projects under Grant No. G19990650. Thanks would like to be given to Dr. T. Hikosaka at the Industrial Research Institute, Aichi Prefectural Government for providing experimental materials.

REFERENCES

- 1) C. McDanel: Metall. Trans. **A16** (1985) 1105–1115.
- 2) D. L. Davidson: Metall. Trans. **A22** (1991) 113–123.
- 3) C. P. You, A. W. Thompson and I. M. Bernstein: Scr. Metall. **21** (1987) 181–185.
- 4) M. Manoharan and J. J. Lewandowski: Acta Metall. Mater. **38** (1990) 489–496.
- 5) H. J. Kim, T. Kobayashi, H. S. Yoon and E. P. Yoon: Mater. Sci. Engng. **A154** (1992) 35–41.
- 6) L. Qian, T. Kobayashi, H. Toda and Z-g. Wang: Mater. Sci. Engng. **A318** (2001) 189–196.
- 7) S. V. Kamat, J. P. Hirth and R. Mehrabian: Acta Metall. **37** (1989) 2395–2402.
- 8) T. Hikosaka, T. Imai and T. Kobayashi: Proceedings of the Sixth Inter. Conf. on Aluminum Alloys, (1998) pp. 1921–1926.
- 9) ASTM-E399-83, Annual Book of ASTM Standards, ASTM, Philadelphia, (1989) p. 487.
- 10) J. R. Rice and M. A. Johnson: *Inelastic Behavior of Solids*, ed. by M. F. Kanninen (McGraw-Hill, New York, 1970) p. 641.
- 11) G. T. Hahn and A. R. Rosenfield: Metall. Trans. **A6** (1975) 653–668.
- 12) D. J. Lloyd: Acta Metall. Mater. **39** (1991) 59–71.
- 13) T. Mochida, M. Taya and D. J. Lloyd: Mater. Trans., JIM **32** (1991) 931–938.
- 14) D. Broek: Engng. Fract. Mech. **5** (1973) 55–66.